A novel GLP-1/GIP dual receptor agonist protects from 6-OHDA lesion in a rat model of Parkinson's disease

Jaishree Jalewa, Mohit Kumar Sharma, Simon Gengler and Christian Hölscher
Division of Biomedical and Life Sciences, Faculty of Health and Medicine, Lancaster University, Lancaster, LA1 4YQ, UK.

Accepted in the journal *Neuropharmacology*

Running title: *a novel dual agonist is neuroprotective*

Corresponding author:
Prof. Christian Hölscher, PhD
Lancaster University
Division of Biomedical and Life Sciences
Faculty of Health and Medicine
Furness college,
Lancaster, LA1 4YQ, UK
+44 (0) 1524 594870
Email: c.holscher@lancaster.ac.uk

Abstract

The incretins glucagon-like peptide 1 (GLP-1) and glucose dependent insulinotropic polypeptide (GIP) are growth factors that have shown neuroprotective effects in animal models of Parkinson's and Alzheimer's disease. In addition, the GLP-1 mimetic exendin-4 has shown protective effects in a clinical trial in Parkinson's disease (PD) patients. GLP-1 analogues are currently on the market as treatments for type II diabetes. We previously showed that the novel dual agonist (DA-JC1) was effective in the 1-methyl-4-phenyl-1,2,3,6-tetrahydropyridine (MPTP) mouse model of PD. Here we demonstrate that DA-JC1 is neuroprotective in the 6-OHDA brain lesion rat model of PD. When treating rats for 6 weeks with DA-JC1 at 25nmol/kg ip once-daily, motor activity as tested in the Rotarod and in the open field was much improved. In the amphetamine and apomorphine circling behaviour tests, the 6-OHDA induced impairments were much reduced by the DA-JC1 treatment. The number of TH positive dopaminergic neurons in the substantia nigra was decreased by 6-OHDA lesion and was increased by DA-JC1 treatment. Dopamine levels in the basal ganglia were reduced by 6-OHDA lesion and increased by DA-JC1. In western blot analysis, levels of the growth factor GDNF and pAkt/CREB cell signaling was enhanced by DA-JC1. The autophagy marker Beclin1 was also activated by the drug. The results demonstrate that dual GLP-1/GIP receptor agonists show promise as a novel treatment for PD.

Keywords: neurodegeneration; brain; insulin; neuroprotection; neuron; incretin

Introduction

Parkinson disease (PD) is the second most common neurodegenerative disease after Alzheimer disease, and current demographic trends show an overall life-time risk close to 4% and predict a doubling of case numbers by 2030 (Schapira, 2013). PD is characterised by a variety of symptoms such as resting tremor, bradykinesia, rigidity and postural instability (Langston, 2002). These symptoms are attributed to the reduction in striatal dopamine levels, which are due to progressive degeneration of dopaminergic neurons in the substantia nigra pars compacta (SNpc) (Moore et al., 2005; Wakamatsu et al., 2008). Several risk factors have been identified, and type 2 diabetes is one of these (Hu et al., 2007; Schernhammer et al., 2011; Sun et al., 2012; Wahlqvist et al., 2012). Previous studies have documented the importance of insulin signaling in the brain (Freiherr et al., 2013; Ghasemi et al., 2013; van der Heide et al., 2006), and observed that insulin signaling is compromised in the brains of patients with PD (Aviles-Olmos et al., 2013b; Moroo et al., 1994; Morris et al., 2011). Analogues of incretin hormones have been developed to improve insulin signaling in type II diabetes (Campbell and Drucker, 2013; Holst, 2004). The main incretin hormones are glucagon-like peptide-1 (GLP-1) and glucose-dependent insulinotropic polypeptide (GIP) (Baggio and Drucker, 2007; Campbell and Drucker, 2013; Doyle and Egan, 2003). We and others have shown that GLP-1 and GIP receptor agonists have shown protective effects in animal models of Alzheimer's disease (Bomfim et al., 2012; Duffy and Holscher, 2013; Faivre and Holscher, 2013a, b; Li et al., 2010; McClean et al., 2011), and clinical trials have started (Hölscher, 2016) with first positive results having been published (Gejl et al., 2016). Importantly, previous investigations found that GLP-1 receptor agonists also showed good neuroprotective effects in different animal models of PD (Bertilsson et al., 2008; Harkavyi et al., 2008; Li et al., 2009; Liu et al., 2015a; Zhang et al., 2015) and showed good effects in a pilot study in PD patients (Aviles-Olmos et al., 2013a; Aviles-Olmos et al., 2014). We have shown good protective effects with GLP-1 and also GIP mimetics in the 1-methyl-4-phenyl-1,2,3,6-tetrahydropypridine (MPTP) mouse model of PD, demonstrating that both receptor pathways show promise to ameliorate disease progression in PD (Li et al., 2015b; Liu et al., 2015a; Liu et al., 2015b; Zhang et al., 2015). The GLP-1 mimetic exendin-4 furthermore showed good effects in the 6-OHDA lesion rat model of PD (Bertilsson et al., 2008; Harkavyi et al., 2008)

Novel dual GLP-1/GIP receptor agonists have been developed to treat type II diabetes and show superior effects to single GLP-1 receptor agonists (Finan et al., 2013). We tested one of these dual agonists (DA-JC1) in the rotenone cell culture model of PD and found that it was protective at a far

lower dose than single GLP-1 or GIP analogues (Jalewa et al., 2016). We furthermore tested the effects of this potent GLP-1/GIP receptor agonist in the MPTP mouse model of PD. We found that DA-JC1 protected mice from the toxic effects of MPTP and reduced loss of motor control, enhanced numbers of TH positive neurons in the substantia nigra, reduced chronic inflammation and apoptotic signaling while enhancing levels of BDNF, a growth factor that protects synapses, and PI3k activity (Cao et al., 2016; Ji et al., 2015). However, animal models of PD do not recapitulate all parameters of PD, and results from these models do not always translate to the clinic (Bove and Perier, 2012; Morin et al., 2014). We therefore tested the DA-JC1 drug in the unilateral 6-OHDA lesion rat model of PD to further investigate if this dual agonist has protective effects in this different chemical lesion animal model.

Materials and Methods

Animals

All animal experiments and procedures were carried out in accordance with the animal handling laws and protocols/procedures approved by the Home Office, London, UK. We used Sprague Dawley male rats in this study that weighed approximately 350-450 gm. The animals were single housed in Individually ventilated cages (IVC's) and had a reverse 12-h light-on-light-off cycle with food and water provided ad libitum. The temperature of the room was set to 21$\pm$ 2 C°. The weight and food intake of animals was registered weekly.

Peptide

The dual agonist DA-JC1 (Peptide Purity: 95.77%) was obtained from the Shanghai Qiangyao Biological Technology (Shanghai, China). The purity of the peptide was confirmed by reversed-phase HPLC and characterised using matrix assisted laser desorption/ionisation time of flight (MALDI-TOF) mass spectrometry.

Peptide sequence of the GLP-1/GIP dual agonist DA-JC1 (Finan et al., 2013):

Y**X**EGTFTSDYSIYLDKQAA**X**EFVNWLLAGGPSSGAPPPS**K**-NH2

X = aminoisobutyric acid; **K** = Lys-γE-C_{16} acyl

Animal Surgery

To increase the selectivity of 6-OHDA towards Dopaminergic neurons, the rats were injected with one intraperitoneal (i.p.) injection with pargyline (5 mg/kg; monoamine oxidase inhibitor) and desipramine (25 mg/kg; noradrenaline uptake inhibitor) 30 min before surgery. The animals were anaesthetised via i.p. injection of Ketamine (100mg/kg body weight) and Xylazine (10mg/kg body weight) and fixed into a stereotaxic frame (WPI International) using ear bars and nose clamp. During the surgery the animal was placed on a heat pad to maintain its body temperature. The skull was shaven and cleaned using alcohol wipes and Betadine Providone Iodine antiseptic solution. A sterile scalpel was used to make a 2 cm incision to expose the skull, followed by measuring and marking the coordinates relative to bregma and drilling a hole at the preferred lesioning site. A fresh vial of 6-OHDA (2mg/ml in 0.01% Ascorbic acid prepared in saline and protected from light and stored at -20 deg C) was used for every lesion and 5µl of this solution was injected at a speed of 1µl/min into the right medial forebrain bundle
(MFB) (Anteroposterior: -2.2, Lateral: -1.5, Dorsoventral: -8.0) using a 10µL Neuro Syringe (Hamilton, Germany) with a 33-gauge needle. In the control group, sham saline was injected with 0.01% Ascorbic acid. The syringe was left in place for 5 min after injection and gently retracted back. The hole in the skull was blocked up using sterile bone-wax (Stoelting, Germany) and the wound closed using 2-3 sutures (Ethilon Nylon sutures, Ethicon). 4% Lidocaine cream was applied near the incision site on the skull followed by Metacam sub-cutaneous pain relief. The rats were placed on a temperature-regulated heated blanket to maintain their body temperature post-recovery and 1ml of sterile water was administered i.p. as soon as the animal showed signs of recovery. After 2-3 hours of recovery from anaesthesia, when mobile and conscious, the animal were returned in their home cage and placed in the IVC rack. The animals with 6-OHDA lesion showed a preference towards the ipsilateral side during recovery. Post-recovery, the animals were fed with apples and soft food for 3 days and their body-weights were recorde and fluid intake was recorded.

Treatment with DA-JC1

Starting 6 days after the 6-OHDA lesion, DA-JC1 was administered at 25nmol/kg ip once-daily for 6 weeks (see Fig. 1).

Apomorphine induced circling test

After 6 weeks of surgery the rats received subcutaneous injection of Apomorphine (Tocris), (0.05mg/kg body weight). 10min after injection, the rats were placed in a clean open-field arena and their activity was recorded by a computerised tracking system (Biosignals, New York) for 40

minutes. The total number of contralateral (opposite the lesioned side) rotations was counted by individuals blind to the experiment.

Amphetamine induced circling test

After 10-12 days of surgery the rats received Methamphetamine hydrochloride (Sigma), i.p. (3mg/kg body weight). After 30min of injection, the rats were placed in a clean open-field arena and their activity was recorded by a computerised tracking system (Biosignals, New York) for 10 minutes. The total number of ipsiversive (towards the lesioned side) rotations was counted by individuals blind to the experiment.

Rotarod Test

Balance and motor coordination was assessed using the Rotarod test (IITC, WPI, UK). Rats were submitted to the rotarod test in the 2nd and 4th week after surgery. Rats were trained on the rotarod twice a day (3 hour inter-trial period) for 3 consecutive days, with the rod accelerating at 10 rpm for 300sec maximum. For the test, the rats were placed on the rotarod that accelerated from 5 to 20 rpm in 20sec and also at 5-45rpm in 200 sec. The latency to fall off and the distance travelled was recorded automatically for a period up to 200sec.

Open Field Test

5 weeks following surgery, the rats were placed in a 150cm diameter, clean, open and well lit arena. The animals were exposed to the arena on two consecutive days for 5 minutes before recording their movement for 10 min on the third day. The animals were recorded by a digital camera. The video was analysed off-line using Ethovision software, Noldus. The arena was cleaned and dried thoroughly before each trial.

Dissection and striatal tissue homogenisation

Rats were deeply anaesthetised with Ketamine and Xylazine, followed by cervical dislocation. After perfusion with 4% PFA solution via the heart, the brains were removed and striata dissected and snap frozen in liquid nitrogen for storage. The striatum was homogenised in phosphate buffered saline (PBS) with protease inhibitor (Roche). For 100mg tissue, 1ml of ice-cold homogenisation buffer was used and later stored at -20ºC overnight. Total protein was extracted by centrifugation at 10,000rpm for 10min and the supernatant collected. Quick start Bradford protein assay reagent (Biorad) was used to quantify the protein concentration in the supernatant.

Striatal Dopamine quantification

The assay was performed in a 96-well plate as per the manufacturer's instructions of the rat dopamine ELISA kit (CUSABIO, USA). Briefly, striatal lysates were diluted 1:2 in the sample diluent and the plates were incubated for 2 hours at 37ºC. After removing the liquid from each well, 100µl of biotin conjugated antibody against dopamine was added to each well and the plate incubated for 1 hour at 37ºC. Each well was aspirated and washed with the wash buffer three times followed by addition of 100µl HRP-avidin antibody and incubated at 37ºC for 1 hour. After washing 5 times, 90µl of TMB substrate was added and the plate incubated for 30min at 37ºC, protected from light. Finally, 50µl of stop solution was added and after gentle mixing, the plate was read at 450nm. The dopamine concentrations were calculated from the standard curve and normalised against total protein.

Western blotting

Lysate containing 2µg of protein was separated on 20-well 4-12% gradient Bis-Tris midi gel with Novex pre-stained marker (Invitrogen) and electrophoresed in running buffer at 180mV for 90min followed by transfer to polyvinylidene difluoride (PVDF) membrane using iBlot® 2 Gel Transfer Device. Following protein transfer, the membrane was washed in 1X TBS-T (tris-buffered saline with 0.05% Tween-20, pH 8) and blocked in 5% skimmed milk for 1hr at 25°C. The membrane was then incubated with anti-pAkt (Ser473) (1:1000) at 4°C overnight and after three washes (5min each) in TBS-T further incubated with 1:2000 horseradish peroxidase-conjugated anti-rabbit IgG. The protein bands were visualized by Amersham ECL Prime western blotting detection reagent according to the manufacturer's instructions. ChemiDoc MP Imaging System with Image Lab software (BIO-RAD) was used to image chemiluminescent bands and perform the analysis of each band intensity. Image Lab™ software controls image capture and optimiszation and produces reports. Beta-actin was used as loading control and relative peak intensity of each marker band analysed on Mac Numbers after normalizing with loading control. To reprobe, the membranes were incubated with Restore stripping buffer (Thermo Scientific, UK) with some agitation for 15min at RT followed by 3 washes in TBS-T for 5min each. The membranes were checked with chemiluminescent detection preceding incubation in another primary antibody of interest.

Perfusion and Immunofluorescence

Eight weeks post surgery, rats were anaesthetised with Ketamine and Xylazine and perfused transcardially with 0.1 M PBS (pH 7.4) buffer followed by ice-cold 4% paraformaldehyde in PBS. The brains were removed and fixed in 4% paraformaldehyde for at least a week and cryoprotected

in a 30% sucrose solution in PBS until the brains sank to the bottom. Brains were then snap frozen using Envirofreez, and coronal sections of 40 µm thickness were cut using a Leica cryostat. Substantia nigra sections were cut according to the rat brain atlas by George Paxinos and Charles Watson (sixth edition). Sections were chosen according to the stereological rules, with the first section taken at random and every seventh section afterward. At least 8-10 sections were taken per immunostaining experiment.

Immunofluorescence (IF) staining for Tyrosine Hydroxylase (TH) immunopositive neurons was performed on the Substantia nigra (SNpc) 40 µm free-floating sections of the following 3 groups: 1. sham saline, 2. 6-OHDA saline and 3. 6-OHDA lesioned, GLP-1/GIP dual agonist treated group. Sections were permeabilised in 0.3% Triton-X 100 in PBS followed by blocking in 5% donkey serum. Staining involved incubating the sections with NB300-110 Sheep Polyclonal Tyrosine Hydroxylase primary antibody (Novus biologicals, 1:500), overnight at 4ºC. Next day, after 3 washes in PBS-T, sections were incubated at room temperature for 1hr with donkey anti-Sheep IgG (H+L) secondary antibody, Alexa Fluor® 488 conjugate (Invitrogen) (1:1000). Sections were cover-slipped with Vectashield mounting medium (Vector laboratories) and sealed with nail polish. Imaging was done on a Zeiss LSM510 Meta Laser Scanning confocal microscope at 488nm wavelength in tiling mode, 3 x 3 tile, 15% overlap.

The numbers of TH-immunospositive neurons in substantial nigra were quantified by applying 2D stereology rules (Bondolfi et al., 2002) by randomly choosing the first section and every third after that. An unbiased dissector was applied randomly to images (x:573.67µm, y:573.67µm.) with 5 brains analysed per group and 3-5 sections per brain. Cells were counted by an operator blind to treatment.

Statistical Analysis

Statistical analysis was done with a two-way ANOVA or one-way ANOVA followed by Bonferroni's Multiple Comparison post-hoc test using the statistics program Prism (Graphpad software, USA). Results are expressed as mean ± standard deviation.

Results

Body weight and food consumption of rats

As GLP-1 analogues can have a weight reducing effect in obese animals and humans (Rodriquez de Fonseca et al., 2000; Wadden et al., 2013), we monitored the weight and food intake. There was no

difference between groups in a three level, two-way ANOVA as shown in fig. 2. N=8 per group.

Amphetamine induced circling test

DA-JC-1 treatment decreased Amphetamine-induced rotations when measured 5 weeks post-lesion. The amphetamine-circling test showed a significant decrease in the ipsilateral rotations of 6-OHDA exposed rats that received DA-JC1 compared with the saline injected 6-OHDA lesioned rats. A 34% decrease ($p<0.05$: One-way ANOVA with Bonferroni post-hoc test) in the number of Amphetamine induced rotations in the DA-JC1 treated group was observed after 4weeks of treatment. A 33.3% decrease ($p<0.05$) in the number of Amphetamine induced rotations in the DA-JC1 treated group was observed when compared to saline treated 6-OHDA lesioned group. An increase of 28% (non-significant) in the number of Amphetamine induced rotations was observed from 1st to 5th week of saline treated group. One-way ANOVA followed by Bonferroni's Multiple Comparison post hoc test, N=8 per group, see fig. 3A.

Apomorphine induced contralateral rotation test

Six weeks post-surgery the rats received subcutaneous injection of apomorphine, (0.05mg/kg body weight). Contralateral rotations were tracked and quantified. The DA-JC1 treatment decreased apomorphine-induced rotations by 89.4% ($p<0.001$) in the contralateral rotations exhibited by the 6-OHDA exposed rats that received DA-JC1 compared with the saline treated ones. One-way ANOVA followed by Bonferroni's Multiple Comparison post hoc test, N=8 per group, see fig. 3B.

Rotarod test

5-45rpm in 200 sec

DA-JC1 treatment improved balance and coordination when tested 2 weeks post-lesion. A significant improvement exhibited in the speed, time and distance by the 6-OHDA lesioned, treated with DA-JC1 group when compared with the saline treated 6-OHDA group. An increase of 17% ($p<0.01$) and 46% ($p<0.01$) was observed in the maximum speed attained on the Rotarod after 2weeks and 4 weeks post-lesion, respectively. An increase of 21% ($p<0.01$) and 76% ($p<0.01$) was observed in the total time on the Rotarod before falling after 2weeks and 4 weeks post-lesion, respectively. A 34% increase ($p<0.05$) and a 2-fold increase was observed in the total distance travelled on the Rotarod after 2weeks and 4 weeks post-lesion, respectively, see fig. 4 top.

5 to 20rpm in 20 sec

The DA-JC1 treatment improved balance and coordination at a slower setting. An increase of 6.3%

($p<0.05$) and 13.5% ($p<0.05$) was observed in the maximum speed attained on the Rotarod after 2 weeks and 4 weeks post-lesion, respectively. An increase of 3-fold ($p<0.0001$) and 4-fold ($p<0.01$) was observed in the total time on the Rotarod before falling after 2 weeks and 4 weeks, respectively. A 4-fold increase ($p<0.0001$) and a 5-fold ($p<0.001$) increase was observed in the total distance travelled on the Rotarod after 2 weeks and 4 weeks, respectively. One-way ANOVA followed by Bonferroni's Multiple Comparison post hoc test, N=8 per group, see fig. 4 bottom.

Open field test

Five weeks post-surgery, animals were put into a 15cm diameter open field and tracked. The number of grooming episodes was significantly reduced after the 6-OHDA lesion ($p<0.05$ compared to sham control) and normalised to control levels by DA-JC1 ($p<0.05$ compared to 6-OHDA lesion group). The number of rearings was not affected by the 6-OHDA lesion. The area covered when traveling was much reduced by 6-OHDA lesion ($p<0.05$ compared to sham control) and normalized to control levels by DA-JC1 ($p<0.05$ compared to the 6-OHDA lesion group). Sample tracks are shown and a 'heat map' representation of overall location distribution which demonstrate that overall motor activity is greatly affected by 6-OHDA lesion is normalised by DA-JC1. One-way ANOVA followed by Bonferroni's Multiple Comparison post hoc test, N=8. See Fig. 5.

Histology

In the immunohistochemical assessment of TH positive neurons in the substantia nigra, it was found that 6-OHDA lesion much reduced the numbers of dopaminergic neurons obtained by 2D stereological analysis in the 6-OHDA injected hemisphere ($p<0.001$ compared to sham control). There was a 58% decrease in number of TH + neurons in the 6-OHDA saline treated group and DA-JC1 increases the number by 37%. There was no difference between the sham control group and the 6-OHDA DA-JC1 treated group. In contrast, there were no differences in neuronal numbers when assessing the contralateral non-lesioned hemisphere. When analysing astrogliosis (GFAP expression), it was found that the 6-OHDA lesion induced robust chronic inflammation ($p<0.0001$ compared to sham saline). DA-JC1 reduced the inflammation ($p<0.01$ compared to sham saline and $p<0.05$ compared to 6-OHDA saline). One-way ANOVA followed by Bonferroni's Multiple Comparison post hoc test; N=5 per group, see fig 6.

Western blot

Analysing the levels of activated Akt compared to total Akt, it was found the 6-OHDA had no

effect on the activation of this growth factor signaling kinase. DA-JC1 treatment increased the levels, though ($p<0.01$ compared to 6-OHDA and $p<0.001$ compared to sham control). CREB activation was much enhanced by DA-JC1 ($p<0.001$ compared to 6-OHDA and sham control). Importantly, the levels of the growth factor GDNF were much enhanced by DA-JC1 ($p<0.01$ compared to 6-OHDA and $p<0.05$ compared to sham control). The levels of the autophagy biomarker beclin1 were also enhanced by DA-JC1 ($p<0.05$ compared to 6-OHDA and sham control). One-way ANOVA followed by Bonferroni's Multiple Comparison post hoc test; N=5 per group, see fig. 7.

Dopamine levels in the basal ganglia

When analysing the dopamine content of basal ganglia tissue by ELISA, it was found that the 6-OHDA injection significantly reduced the levels ($p<0.0001$ compared to sham controls). Treatment of lesioned animals with DA-JC1 increased the dopamine levels compared to 6-OHDA saline treated brains ($p<0.05$). N=6 per group, see fig. 8. One-way ANOVA with Bonferroni's post-hoc test.

Discussion

The results demonstrate that the novel GLP-1/GIP dual receptor agonist DA-JC1 has Neuroprotective properties in the 6-OHDA lesion rat model. The 6-OHDA unilateral lesion induced circling behaviour which was emphasised by apomorphine or amphetamine by modulating dopaminergic transmission. DA-JC1 much reduced circling behaviour, indicating that dopaminergic transmission was improved by the drug. Similar observations were made in the Rotarod and the open field tests where performance was improved by DA-JC1. The histology confirmed that DA-JC1 protected dopaminergic neurons from 6-OHDA toxicity. Furthermore, the levels of dopamine measured in the basal ganglia were much reduced by 6-OHDA, and nearly normalised by DA-JC1 treatment. DA-JC1 treatment also enhanced the growth-factor signaling associated kinase Akt in 6-OHDA treated rats. Akt signaling activates neuroprotective cellular processes and gene expression in PD, and gene variations are a risk factor for PD (Xiromerisiou et al., 2008). We have previously shown that Akt was also activated by GLP-1 receptor agonists in the MPTP mouse model of PD (Liu et al., 2015b) and by the DA-JC1 (Ji et al., 2015). Activation of CREB, a key regulator of gene expression, also contributes to neuroprotection (Li et al., 2015b; Sharma et al., 2013). The growth

factor Glial-Derived Neurotrophic Factor (GDNF) was expressed at a higher level, which may explain the protection of dopaminergic neurons. GDNF has been identified as the key growth factor for dopaminergic neurons which enhances cell repair and regeneration (Allen et al., 2013; Broome et al., 1999). Interestingly, the autophagy biomarker Beclin1 was enhanced by DA-JC1 treatment. Autophagy is a key mechanism to eliminate cellular waste and misfolded proteins to protect the cell (Jang et al., 2014). It has been shown that autophagy is one of the cellular systems that are impaired in PD, and that can enhance neuronal survival (Ghavami et al., 2014; Zhang et al., 2013). We had previously shown in an *in vitro* study that autophagy is activated by GLP-1 and GIP analogues (Jalewa et al., 2016), and our findings in the present study confirm that this is also the case *in vivo*. Importantly, chronic astrogliosis was reduced by DA-JC1, which may contribute to the overall neuroprotective effects. Chronic inflammation is a key factor in PD disease progression (Tansey and Goldberg, 2010). We have previously shown in the MPTP mouse model of PD that astrogliosis and microglia activation is reduced by DA-JC1 (Cao et al., 2016), so our findings in the present study confirm the anti-inflammatory properties of GLP-1 and GIP.

In conclusion, the protective results obtained with DA-JC1 in the 6-OHDA rat model of PD mirror those we observed in the MPTP mouse model of PD. We observed protection of motor activity in the Rotarod and open field, reduced loss of TH positive neurons in the SN, a reduction of chronic inflammation in the brain, enhanced BDNF expression, and protection of synapses (Cao et al., 2016; Ji et al., 2015). It is encouraging that the distinct improvement in key biomarkers of growth factor signaling, apoptosis and inflammation are observed in two different PD animal models. We furthermore found protective effects of DA-JC1 in a mouse model of stroke (Han et al., 2015). The observed protective effects also confirm the neuroprotective effects of the GLP-1 mimetic exendin-4 in the 6-OHDA rat model as reported by others (Bertilsson et al., 2008; Harkavyi et al., 2008). Another study testing the GLP-1 analogue liraglutide did not find neuroprotective effects in the 6-OHDA rat model (Hansen et al., 2016). This is most likely due to technical differences in the study design. For example, in that study, the authors only started to treat the animals with liraglutide 6 weeks post- 6-OHDA injection in one experiment. It is well known that the dopaminergic neurons will have died after 2 weeks post-6-OHDA lesion (Falcone et al., 2015), so no effect of liraglutide was to be expected under those conditions.

We have previously tested a wide range of incretin analogues in the MPTP mouse model of PD. When comparing the more effective GLP-1 mimetics liraglutide and lixisenatide with the older drug exendin-4, it was found that both liraglutide and lixisenatide showed superior protective effects over exendin-4. Motor activity was partly rescued by both drugs, and dopaminergic neurons were protected in the substantia nigra. Expression of the dopamine biomarker tyrosine hydroxylase

(TH) was also rescued in the liraglutide and lixisenatide treated mice. Pro-apoptotic cell signaling was reduced, while growth factor signaling was enhanced by both drugs (Liu et al., 2015a). This result was confirmed when testing the GLP-1 analogue (Val8)GLP-1-Glu-PAL, a new version of liraglutide with a longer biological half-life (Zhang et al., 2015). Testing the dual GLP-1/glucagon receptor agonist D-Ser2-oxyntomodulin furthermore showed similar neuroprotective effects (Liu et al., 2015b). When testing the incretin GIP, we found that the long-lasting protease resistant analogue D-Ala2-GIP-glu-PAL showed good protective effects. Motor activity was partly rescued, and the number of dopaminergic neurons in the substantia nigra was increased. Synapse numbers were increased, and the cAMP/PKA/CREB growth factor signaling pathway was activated by D-Ala2-GIP-glu-PAL (Li et al., 2015b). We and others also found good neuroprotective effects of GLP-1 and GIP mimetics in mouse models of Alzheimer's disease (Cai et al., 2014; Faivre and Holscher, 2013b; Li et al., 2010; McClean and Holscher, 2014; Perry and Greig, 2005), and others found neuroprotective effects of GLP-1 mimetics in traumatic brain injury (Eakin et al., 2013; Li et al., 2015a). These studies demonstrate that both GLP-1 and GIP signaling pathways show promising protective effects by activating growth factor signaling pathways, reducing inflammation, re-sensitising insulin signaling in the brain and normalising energy utilisation (Holscher, 2014). Therefore, the development of novel dual GLP-1/GIP agonists are a promising new development that may show even better protection than single incretin analogues. In diabetes drug research, novel dual agonists such as DA-JC1 have shown superior effects compared to lirglutide (Finan et al., 2013). We now have shown promising neuroprotective effects of DA-JC1 in two different animal models of PD (Cao et al., 2016; Ji et al., 2015). Newer dual agonists are currently being tested and directly compared with liraglutide, the currently best GLP-1 analogue on the market (Hölscher, 2016).

As the GLP-1 mimetics exendin-4 and liraglutide are already on the market to treat diabetes, clinical trials have started that investigate the neuroprotective effects of exendin-4 or liraglutide in PD or AD patients. A pilot trial of exendin-4 in PD patients has shown good effects (clinical trials identifier NCT01174810). This 'proof of concept' study tested the effects of exendin-4 in an open label trial in 45 patients. When assessing motor activity in these patients, clear improvements had been observed, and even cognition was improved as measured by the specifically designed Mattis DRS-2 cognitive test. Patients were re-tested 12 months after the trial had finished, and the differences between groups in motor performance and cognitive scores had not changed (Aviles-Olmos et al., 2014). This suggests that the group difference is not due to a placebo effect, as 12 months is too long for such subjective effects to last. Based on these encouraging results, a phase II clinical trial that tested the once-weekly formulation of exendin-4, Bydureon®, has been completed

(NCT01971242). The results have not been published at this stage. A phase II trial testing liraglutide in PD patients has started in August 2016, testing patients in a double blind, placebo controlled design for one year.

Clinical trials of novel dual GLP-1/GIP analogues in diabetes patients are ongoing, and the available data show that these drugs are effective and safe to take (Finan et al., 2013; Finan et al., 2015). Once these drugs are licenced for use in patients, they can be fast-tracked into clinical trials in PD patients, with the hope of stopping disease progression in its tracks (Hölscher, 2016).

Acknowledgements

The research had been supported by a grant of the Cure Parkinson's Trust UK. CH is a named inventor on a patent application that list dual GLP-1/GIP analogues as novel treatments for AD or PD. The patents application is owned by Lancaster University. The other authors do not declare a conflict of interest.

References

Allen, S. J., Watson, J. J., Shoemark, D. K., Barua, N. U., Patel, N. K., 2013. GDNF, NGF and BDNF as therapeutic options for neurodegeneration. Pharmacol Ther 138, 155-175.

Aviles-Olmos, I., Dickson, J., Kefalopoulou, Z., Djamshidian, A., Ell, P., Soderlund, T., Whitton, P., Wyse, R., Isaacs, T., Lees, A., Limousin, P., Foltynie, T., 2013a. Exenatide and the treatment of patients with Parkinson's disease. J Clin Invest 123, 2730-2736.

Aviles-Olmos, I., Dickson, J., Kefalopoulou, Z., Djamshidian, A., Kahan, J., Fmedsci, P. E., Whitton, P., Wyse, R., Isaacs, T., Lees, A., Limousin, P., Foltynie, T., 2014. Motor and Cognitive Advantages Persist 12 Months After Exenatide Exposure in Parkinson's Disease. J Parkinsons Dis 4, 337-344.

Aviles-Olmos, I., Limousin, P., Lees, A., Foltynie, T., 2013b. Parkinson's disease, insulin resistance and novel agents of neuroprotection. Brain 136, 374-384.

Baggio, L. L., Drucker, D. J., 2007. Biology of incretins: GLP-1 and GIP. Gastroenterology 132, 2131-2157.

Bertilsson, G., Patrone, C., Zachrisson, O., Andersson, A., Dannaeus, K., Heidrich, J., Kortesmaa, J., Mercer, A., Nielsen, E., Ronnholm, H., Wikstrom, L., 2008. Peptide hormone exendin-4 stimulates subventricular zone neurogenesis in the adult rodent brain and induces recovery in an animal model of Parkinson's disease. J Neurosci Res 86, 326-338.

Bomfim, T. R., Forny-Germano, L., Sathler, L. B., Brito-Moreira, J., Houzel, J. C., Decker, H., Silverman, M. A., Kazi, H., Melo, H. M., McClean, P. L., Holscher, C., Arnold, S. E., Talbot, K., Klein, W. L., Munoz, D. P., Ferreira, S. T., De Felice, F. G., 2012. An anti-diabetes agent protects the mouse brain from defective insulin signaling caused by Alzheimer's disease-associated Abeta oligomers. J Clin Invest 122, 1339-1353.

Bondolfi, L., Calhoun, M., Ermini, F., Kuhn, H. G., Wiederhold, K. H., Walker, L., Staufenbiel, M., Jucker, M., 2002. Amyloid-associated neuron loss and gliogenesis in the neocortex of amyloid precursor protein transgenic mice. J Neurosci 22, 515-522.

Bove, J., Perier, C., 2012. Neurotoxin-based models of Parkinson's disease. Neuroscience 211, 51-76.

Broome, J. D., Wills, K. V., Lapchak, P. A., Ghetti, B., Camp, L. L., Bayer, S. A., 1999. Glial cell line-derived neurotrophic factor protects midbrain dopamine neurons from the lethal action of the weaver gene: a quantitative immunocytochemical study. Brain Res Dev Brain Res 116, 1-7.

Cai, H. Y., Holscher, C., Yue, X. H., Zhang, S. X., Wang, X. H., Qiao, F., Yang, W., Qi, J. S., 2014. Lixisenatide rescues spatial memory and synaptic plasticity from amyloid beta protein-induced impairments in rats. Neuroscience 277C, 6-13.

Campbell, J. E., Drucker, D. J., 2013. Pharmacology, physiology, and mechanisms of incretin hormone action. Cell Metab 17, 819-837.

Cao, L., Li, D., Feng, P., Li, L., Xue, G., Li, G., Hölscher, C., 2016. A novel dual GLP-1 and GIP incretin receptor agonist is neuroprotective in a mouse model of Parkinson's disease by reducing chronic inflammation in the brain. Neuroreport 37, 384-391.

Doyle, M. E., Egan, J. M., 2003. Pharmacological agents that directly modulate insulin secretion. Pharmacol. Rev. 55, 105-131.

Duffy, A. M., Holscher, C., 2013. The incretin analogue D-Ala(2)GIP reduces plaque load, astrogliosis and oxidative stress in an APP/PS1 mouse model of Alzheimer's disease. Neuroscience 228, 294-300.

Eakin, K., Li, Y., Chiang, Y. H., Hoffer, B. J., Rosenheim, H., Greig, N. H., Miller, J. P., 2013. Exendin-4 ameliorates traumatic brain injury-induced cognitive impairment in rats. PLoS One 8, e82016.

Faivre, E., Holscher, C., 2013a. D-Ala2GIP facilitated synaptic plasticity and reduces plaque load in aged wild type mice and in an Alzheimer's disease mouse model. J Alzheimers Dis 35, 267-283.

Faivre, E., Holscher, C., 2013b. Neuroprotective effects of D-Ala2GIP on Alzheimer's disease biomarkers in an APP/PS1 mouse model. Alzheimers Res Ther 5, 20-28.

Falcone, R., Florio, T. M., Di Giacomo, E., Benedetti, E., Cristiano, L., Antonosante, A., Fidoamore, A., Massimi, M., Alecci, M., Ippoliti, R., Giordano, A., Cimini, A., 2015. PPARbeta/delta and gamma in a rat model of Parkinson's disease: possible involvement in PD symptoms. J Cell Biochem 116, 844-855.

Finan, B., Ma, T., Ottaway, N., Muller, T. D., Habegger, K. M., Heppner, K. M., Kirchner, H., Holland, J., Hembree, J., Raver, C., Lockie, S. H., Smiley, D. L., Gelfanov, V., Yang, B., Hofmann, S., Bruemmer, D., Drucker, D. J., Pfluger, P. T., Perez-Tilve, D., Gidda, J., Vignati, L., Zhang, L., Hauptman, J. B., Lau, M., Brecheisen, M., Uhles, S., Riboulet, W., Hainaut, E., Sebokova, E., Conde-Knape, K., Konkar, A., DiMarchi, R. D., Tschop, M. H., 2013. Unimolecular dual incretins maximize metabolic benefits in rodents, monkeys, and humans. Sci Transl Med 5, 209ra151.

Finan, B., Yang, B., Ottaway, N., Smiley, D. L., Ma, T., Clemmensen, C., Chabenne, J., Zhang, L., Habegger, K. M., Fischer, K., Campbell, J. E., Sandoval, D., Seeley, R. J., Bleicher, K., Uhles, S., Riboulet, W., Funk, J., Hertel, C., Belli, S., Sebokova, E., Conde-Knape, K., Konkar, A., Drucker, D. J., Gelfanov, V., Pfluger, P. T., Muller, T. D., Perez-Tilve, D., DiMarchi, R. D., Tschop, M. H., 2015. A rationally designed monomeric peptide triagonist corrects obesity and diabetes in rodents. Nat Med 21, 27-36.

Freiherr, J., Hallschmid, M., Frey, W. H., 2nd, Brunner, Y. F., Chapman, C. D., Holscher, C., Craft, S., De Felice, F. G., Benedict, C., 2013. Intranasal insulin as a treatment for Alzheimer's disease: a review of basic research and clinical evidence. CNS Drugs 27, 505-514.

Gejl, M., Gjedde, A., Egefjord, L., Møller, A., Hansen, S. B., Vang, K., Rodell, A. B., Braendgaard, H., Gottrup, H., Schacht, A., Møller, N., Brock, B., Rungby, J., 2016. In Alzheimer's Disease, Six-Month Treatment with GLP-1 Analogue Prevents Decline of Brain Glucose Metabolism: Randomized, Placebo-Controlled, Double-Blind Clinical Trial. Front Aging Neurosci 8, 1-10.

Ghasemi, R., Dargahi, L., Haeri, A., Moosavi, M., Mohamed, Z., Ahmadiani, A., 2013. Brain insulin dysregulation: implication for neurological and neuropsychiatric disorders. Mol Neurobiol 47, 1045-1065.

Ghavami, S., Shojaei, S., Yeganeh, B., Ande, S. R., Jangamreddy, J. R., Mehrpour, M., Christoffersson, J., Chaabane, W., Moghadam, A. R., Kashani, H. H., Hashemi, M., Owji, A. A., Los, M. J., 2014. Autophagy and apoptosis dysfunction in neurodegenerative disorders. Prog Neurobiol 112, 24-49.

Han, L., Holscher, C., Xue, G. F., Li, G., Li, D., 2015. A novel dual-glucagon-like peptide-1 and glucose-dependent insulinotropic polypeptide receptor agonist is neuroprotective in transient focal cerebral ischemia in the rat. Neuroreport 27, 23-32.

Hansen, H. H., Fabricius, K., Barkholt, P., Mikkelsen, J. D., Jelsing, J., Pyke, C., Knudsen, L. B., Vrang, N., 2016. Characterization of liraglutide, a glucagon-like peptide-1 (GLP-1) receptor agonist, in rat partial and full nigral 6-hydroxydopamine lesion models of Parkinson's disease. Brain Res 1646, 354-365.

Harkavyi, A., Abuirmeileh, A., Lever, R., Kingsbury, A. E., Biggs, C. S., Whitton, P. S., 2008. Glucagon-like peptide 1 receptor stimulation reverses key deficits in distinct rodent models of Parkinson's disease. J Neuroinflammation 5, 19(11-19).

Holscher, C., 2014. Insulin, incretins and other growth factors as potential novel treatments for Alzheimer's and Parkinson's diseases. Biochem Soc Trans 42, 593-599.

Hölscher, C., 2016. GLP-1 and GIP analogues as novel treatments for Alzheimer's and Parkinson's disease. Cardiovasc Endocrinol 5, 93-98.

Holst, J. J., 2004. Treatment of type 2 diabetes mellitus with agonists of the GLP-1 receptor or DPP-IV inhibitors. Expert Opin Emerg Drugs 9, 155-166.

Hu, G., Jousilahti, P., Bidel, S., Antikainen, R., Tuomilehto, J., 2007. Type 2 diabetes and the risk of Parkinson's disease. Diabetes Care 30, 842-847.

Jalewa, J., Sharma, M. K., Holscher, C., 2016. Novel incretin analogues improve autophagy and protect from mitochondrial stress induced by rotenone in SH-SY5Y cells. J Neurochem 139, 55-67.

Jang, W., Kim, H. J., Li, H., Jo, K. D., Lee, M. K., Song, S. H., Yang, H. O., 2014. 1,25-Dyhydroxyvitamin D(3) attenuates rotenone-induced neurotoxicity in SH-SY5Y cells through induction of autophagy. Biochem Biophys Res Commun 451, 142-147.

Ji, C., Xue, G. F., Lijun, C., Feng, P., Li, D., Li, L., Li, G., Holscher, C., 2015. A novel dual GLP-1 and GIP receptor agonist is neuroprotective in the MPTP mouse model of Parkinson's disease by increasing expression of BNDF. Brain Res 1634, 1-11.

Langston, J. W., 2002. Parkinson's disease: current and future challenges. Neurotoxicology 23, 443-450.

Li, Y., Bader, M., Tamargo, I., Rubovitch, V., Tweedie, D., Pick, C. G., Greig, N. H., 2015a. Liraglutide is neurotrophic and neuroprotective in neuronal cultures and mitigates mild traumatic brain injury in mice. J Neurochem 135, 1203-1217.

Li, Y., Duffy, K., Ottinger, M., Ray, B., Bailey, J., Holloway, H., Tweedie, D., Perry, T., Mattson, M., Kapogiannis, D., Sambamurti, K., Lahiri, D., Greig, N., 2010. GLP-1 Receptor Stimulation

Reduces Amyloid-beta Peptide Accumulation and Cytotoxicity in Cellular and Animal Models of Alzheimer's Disease. J Alzheimers Dis 19, 1205-1219.

Li, Y., Liu, W., Li, L., Holscher, C., 2015b. Neuroprotective effects of a GIP analogue in the MPTP Parkinson's disease mouse model. Neuropharmacology 101, 255-263.

Li, Y., Perry, T., Kindy, M. S., Harvey, B. K., Tweedie, D., Holloway, H. W., Powers, K., Shen, H., Egan, J. M., Sambamurti, K., Brossi, A., Lahiri, D. K., Mattson, M. P., Hoffer, B. J., Wang, Y., Greig, N. H., 2009. GLP-1 receptor stimulation preserves primary cortical and dopaminergic neurons in cellular and rodent models of stroke and Parkinsonism. Proc Natl Acad Sci U S A 106, 1285-1290.

Liu, W., Jalewa, J., Sharma, M., Li, G., Li, L., Hölscher, C., 2015a. Neuroprotective effects of lixisenatide and liraglutide in the MPTP mouse model of Parkinson's disease. Neuroscience 303, 42-50.

Liu, W., Li, Y., Jalewa, J., Saunders-Wood, T., Li, L., Holscher, C., 2015b. Neuroprotective effects of an oxyntomodulin analogue in the MPTP mouse model of Parkinson's disease. Eur J Pharmacol 765, 284-290.

McClean, P., Parthsarathy, V., Faivre, E., Hölscher, C., 2011. The diabetes drug Liraglutide prevents degenerative processes in a mouse model of Alzheimer's disease. J Neurosci 31, 6587-6594.

McClean, P. L., Holscher, C., 2014. Lixisenatide, a drug developed to treat type 2 diabetes, shows neuroprotective effects in a mouse model of Alzheimer's disease. Neuropharmacology 86C, 241-258.

Moore, D. J., West, A. B., Dawson, V. L., Dawson, T. M., 2005. Molecular pathophysiology of Parkinson's disease. Annu Rev Neurosci 28, 57-87.

Morin, N., Jourdain, V. A., Di Paolo, T., 2014. Modeling dyskinesia in animal models of Parkinson disease. Exp Neurol 256, 105-116.

Moroo, I., Yamada, T., Makino, H., Tooyama, I., McGeer, P. L., McGeer, E. G., Hirayama, K., 1994. Loss of insulin receptor immunoreactivity from the substantia nigra pars compacta neurons in Parkinson's disease. Acta Neuropathol (Berl) 87, 343-348.

Morris, J. K., Bomhoff, G. L., Gorres, B. K., Davis, V. A., Kim, J., Lee, P. P., Brooks, W. M., Gerhardt, G. A., Geiger, P. C., Stanford, J. A., 2011. Insulin resistance impairs nigrostriatal dopamine function. Exp Neurol 231, 171-180.

Perry, T., Greig, N. H., 2005. Enhancing central nervous system endogenous GLP-1 receptor pathways for intervention in Alzheimer's disease. Curr Alzheimer Res 2, 377-385.

Rodriquez de Fonseca, F., Navarro, M., Alvarez, E., Roncero, I., Chowen, J. A., Maestre, O., Gomez, R., Munoz, R. M., Eng, J., Blazquez, E., 2000. Peripheral versus central effects of glucagon-like peptide-1 receptor agonists on satiety and body weight loss in Zucker obese rats. Metabolism 49, 709-717.

Schapira, A. H., 2013. Recent developments in biomarkers in Parkinson disease. Curr Opin Neurol 26, 395-400.

Schernhammer, E., Hansen, J., Rugbjerg, K., Wermuth, L., Ritz, B., 2011. Diabetes and the risk of developing Parkinson's disease in Denmark. Diabetes Care 34, 1102-1108.

Sharma, M., Jalewa, J., Holscher, C., 2013. Neuroprotective and anti-apoptotic effects of Liraglutide on SH-SY5Y cells exposed to Methylglyoxal stress. J Neurochem 128, 459-471.

Sun, Y., Chang, Y. H., Chen, H. F., Su, Y. H., Su, H. F., Li, C. Y., 2012. Risk of Parkinson disease onset in patients with diabetes: a 9-year population-based cohort study with age and sex stratifications. Diabetes Care 35, 1047-1049.

Tansey, M. G., Goldberg, M. S., 2010. Neuroinflammation in Parkinson's disease: its role in neuronal death and implications for therapeutic intervention. Neurobiol Dis 37, 510-518.

van der Heide, L. P., Ramakers, G. M., Smidt, M. P., 2006. Insulin signaling in the central nervous system: learning to survive. Prog Neurobiol 79, 205-221.

Wadden, T., Hollander, P., Klein, S., Niswender, K., Woo, V., Hale, P. M., Aronne, L., 2013. Weight maintenance and additional weight loss with liraglutide after low-calorie diet-induced weight loss: the SCALE Maintenance randomized study. Int J Obes (Lond) 37, 1443-1451.

Wahlqvist, M. L., Lee, M. S., Hsu, C. C., Chuang, S. Y., Lee, J. T., Tsai, H. N., 2012. Metformin-inclusive sulfonylurea therapy reduces the risk of Parkinson's disease occurring with Type 2 diabetes in a Taiwanese population cohort. Parkinsonism Relat Disord 18, 753-758.

Wakamatsu, M., Iwata, S., Funakoshi, T., Yoshimoto, M., 2008. Dopamine receptor agonists reverse behavioral abnormalities of alpha-synuclein transgenic mouse, a new model of Parkinson's disease. J Neurosci Res 86, 640-646.

Xiromerisiou, G., Hadjigeorgiou, G. M., Papadimitriou, A., Katsarogiannis, E., Gourbali, V., Singleton, A. B., 2008. Association between AKT1 gene and Parkinson's disease: a protective haplotype. Neurosci Lett 436, 232-234.

Zhang, S., Xue, Z. F., Huang, L. P., Fang, R. M., He, Y. P., Li, L., Fang, Y. Q., 2013. Dynamic expressions of Beclin 1 and tyrosine hydroxylase in different areas of 6-hydroxydopamine-induced Parkinsonian rats. Cell Mol Neurobiol 33, 973-981.

Zhang, Y. F., Chen, Y. M., LI, L., Hölscher, C., 2015. Neuroprotective effects of (Val8)GLP-1-Glu-PAL in the MPTP Parkinson's disease mouse model. Behav Brain Res 293, 107-113.

Figure captions

Fig. 1: Schematic diagram of the experimental design shows that rats received an injection of Desipramine and Pargyline 1 day prior to the surgery followed by a stereotaxic injection of 6-OHDA or Saline in the MFB of right hemisphere. Six days later it was followed by daily injection of DA-JC1 i.p. (25nmol/kg body weight) for a total of 6 weeks. Amphetamine induced-circling tests were performed on the rats at 1 week and 5 weeks along with apomorphine induced contralateral rotational tests at 6 weeks. Rotarod was performed at 2 and 4 weeks and Open field test after 5 weeks. The rats were transcardially perfused using 4% Paraformaldehyde and the brains dissected out to be used for Immunohistochemistry and western blotting performed on lysate generated from striatum tissue dissected from non-perfused rats.

Fig. 2: Body weight of animals of the three groups. Treatment with 6-OHDA + saline or with 6-OHDA + DA-JC1 did not affect body weight over time (two-way ANOVA). Error bars are SD, N=8 per group.

Fig. 3: A. Amphetamine-induced circling. Animals received methamphetamine hydrochloride i.p. (3mg/kg body weight). After 30min of injection, the rats were placed in an open-field arena and their activity was recorded for 10 minutes. B. Apomorphine- induced circling. After 6 weeks of surgery the rats received subcutaneous injection of Apomorphine (Tocris), (0.05mg/kg body weight). 10min after injection the rats were placed in an open field and their activity was recorded for 45 minutes. Error bars are SD, N=8 per group. One-way ANOVA with Bonferroni post-hoc tests, ***=$p < 0.001$, *=$p<0.05$, ns: non-significant.

Fig. 4: Rotarod performance. Animals were tested in the Rotarod at week 2 and 4 at two settings, 5-45rpm increase over 200 sec (top) and 5-20rpm over 20 sec (bottom). The 6-OHDA lesion impaired animals in this motor competency task. DA-JC1 treatment improved the animals' performance after the lesion. Performance at the 5-20rpm over 20 sec setting was not different to controls in the drug group. Error bars are SD, N=8 per group, ****=$p < 0.0001$, ***=$p < 0.001$, **=$p<0.01$, *=$p<0.05$, ns: non-significant.

Fig. 5: Open field behavior. Grooming activity is reduced by the 6-OHDA lesion and normalised by DA-JC1 treatment. No effect was seen on rearing activity. The overall distance covered was reduced by the 6-OHDA lesion and normalised by DA-JC1. Sample tacks and a heat map of distribution of location is shown. Error bars are SD, N=8, *=$p<0.05$, ns: non-significant.

Fig. 6: Histology of TH+ and GFAP positive neurons in the substantia nigra. A: When quantifying the tyrosine hydroxylase (TH) positive neurons that produce dopamine, it was found that the 6-OHDA lesion reduced neuronal numbers. DA-JC1 protected neurons from the lesion. B: Inflammation was increased by 6-OHDA as shown be enhanced GFAP expression in astroglia. DA-JC1 reduced the chronic inflammation. Error bars are SD. N=5 per group, ****=$p < 0.0001$, ***=$p < 0.001$, **=$p<0.01$, *=$p<0.05$, ns: non-significant.

Fig. 7: Western blot analysis of key biomarkers in the brain (n=5). a. Ratio of pAkt (Ser473)/panAkt: There is a significant increase of 71.4% ($p<0.01$) in the pAkt (Ser473)/panAkt expression in the 6-OHDA + DA-JC1 treated group as compared to the 6-OHDA + saline treated group; b. Ratio of pCREB/Total CREB: DA-JC1 treatment increases pCREB expression by 2.2 fold and 2-fold when compared to the saline treated sham and 6-OHDA groups; c. Ratio of GDNF/beta-actin: a 1.3-fold and 1.4-fold increase increase in GDNF expression in the 6-OHDA DA group as

compared to sham saline and 6-OHDA saline group; d. Ratio of Beclin/beta-actin: DA treatment enhances autophagy as evident from 1.54-fold and 1.5-fold increase in the Beclin- 1 expression in 6-OHDA DA group as compared to the sham saline and 6-OHDA saline group, respectively. Error bars are STD. N=5 per group, ***=$p < 0.001$, **=$p<0.01$, *=$p<0.05$, ns: non-significant.

Fig. 8: Dopamine content in the ipsilateral striatum of Sham Saline, 6-OHDA Saline and 6-OHDA + DA-JC1 groups. Stereotaxic administration of 6-OHDA in the MFB of the right hemisphere resulted in a decrease of 52% in the dopamine levels in the striatum. This decrease was ameliorated by DA-JC1 treatment, which increased the dopamine content by 56% in the 6-OHDA + DA-JC1 group as compared to the 6-OHDA saline treated group. Error bars are SD, N=6 per group. (****=$p<0.0001$, *=$p<0.05$, ns: non-significant).

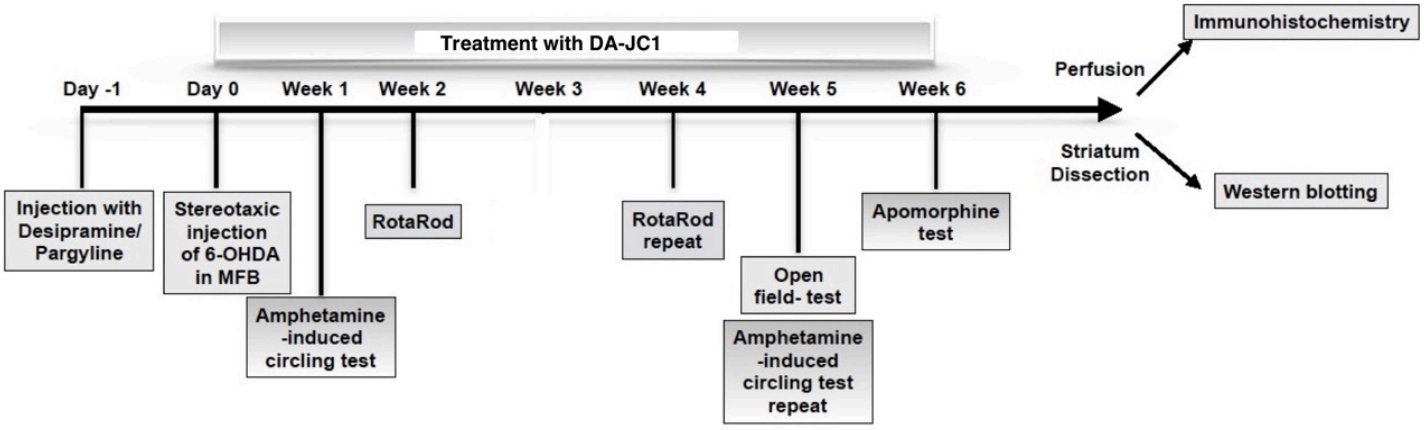
Treatment with DA-JC1
Day -1
Day 0
Week 1
Week 2
Week 3
Week 4
Week 5
Week 6
Perfusion
Immunohistochemistry
Striatum Dissection
Western blotting
Injection with Desipramine/ Pargyline
Stereotaxic injection of 6-OHDA in MFB
Amphetamine -induced circling test
RotaRod
RotaRod repeat
Open field- test
Amphetamine -induced circling test repeat
Apomorphine test

Fig. 1

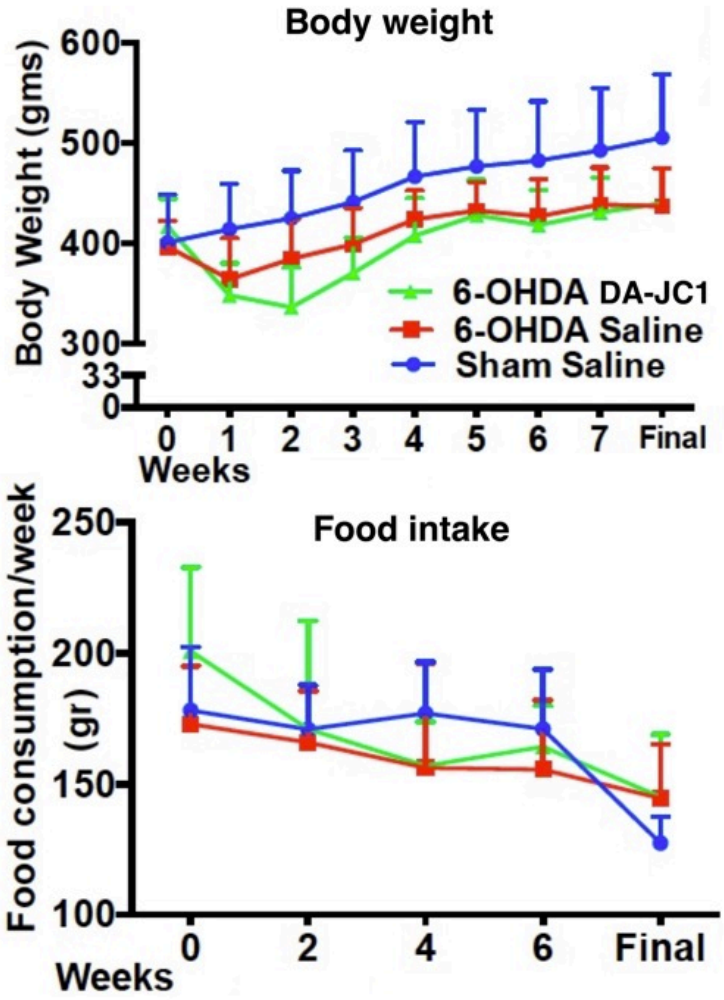
Body weight
Body Weight (gms)
600
500
400
300
33
0
0 1 2 3 4 5 6 7 Final
Weeks
6-OHDA DA-JC1
6-OHDA Saline
Sham Saline
Food intake
Food consumption/week (gr)
250
200
150
100
0 2 4 6 Final
Weeks

Fig. 2

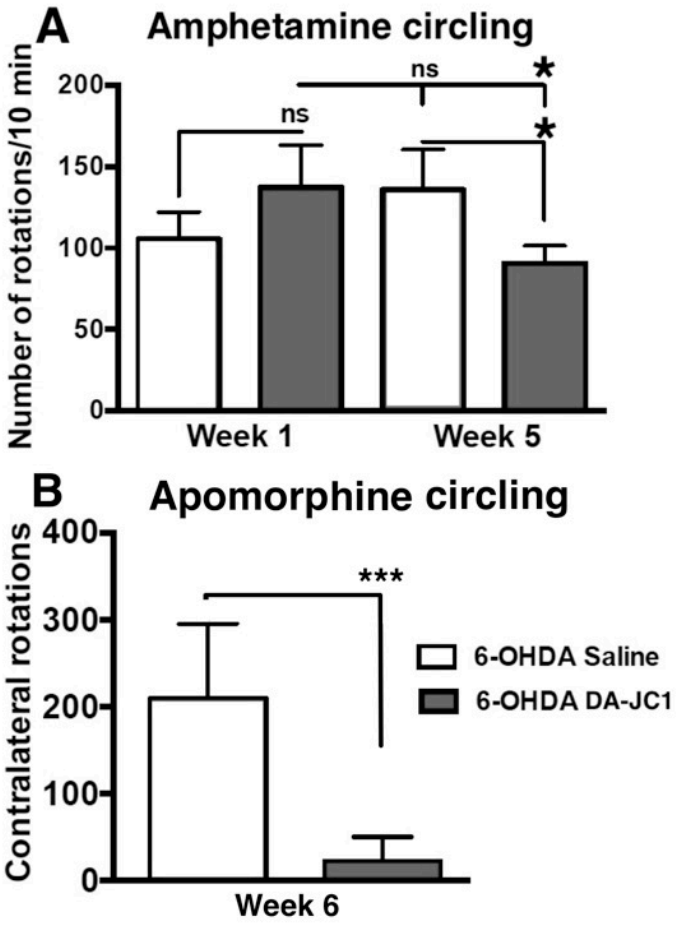
A
Amphetamine circling
Number of rotations/10 min
200
150
100
50
0
ns
ns
*
*
Week 1
Week 5
B
Apomorphine circling
Contralateral rotations
400
300
200
100
0
***
6-OHDA Saline
6-OHDA DA-JC1
Week 6

Fig. 3

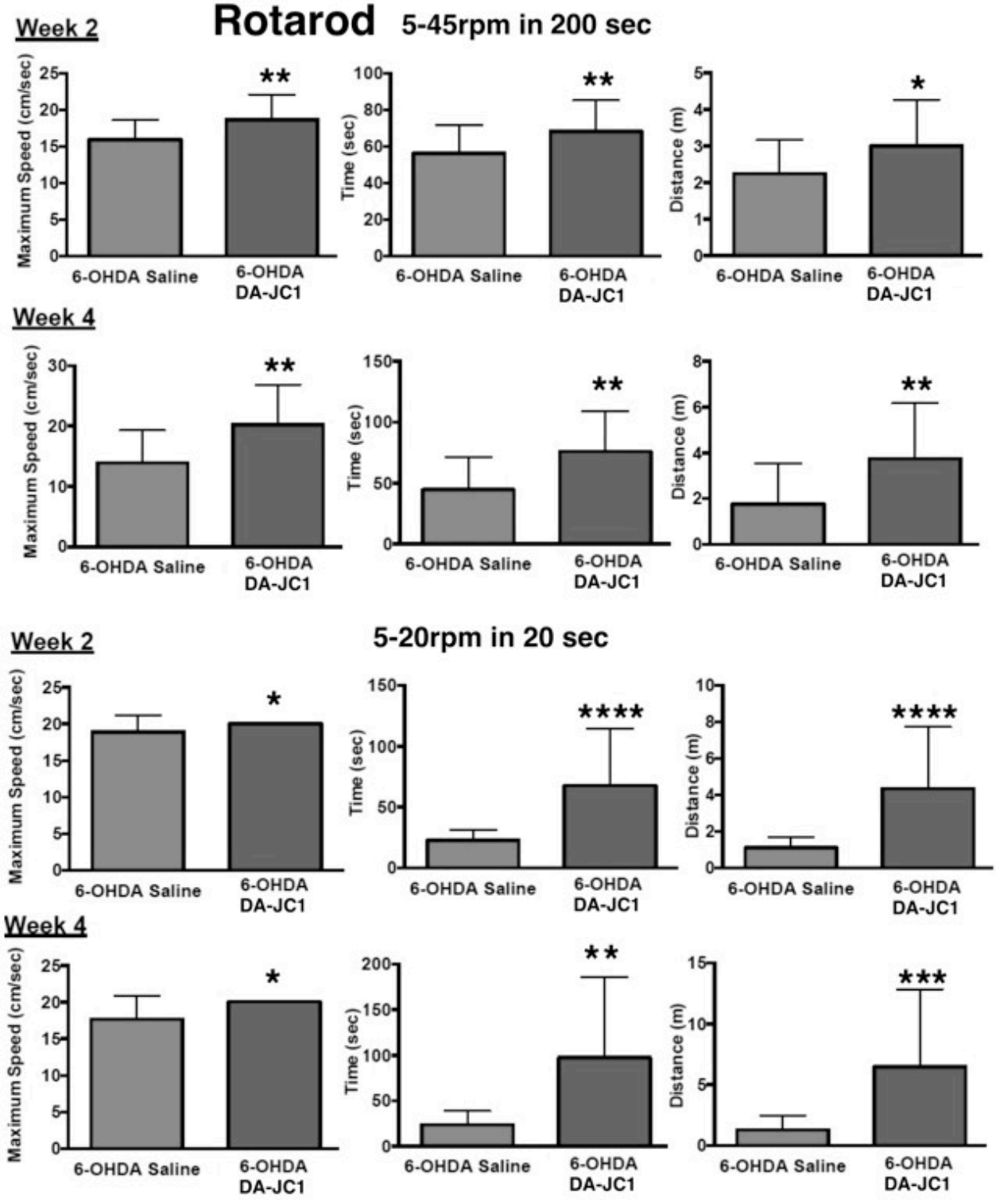
Week 2
Rotarod 5-45rpm in 200 sec
Maximum Speed (cm/sec)
Time (sec)
Distance (m)
6-OHDA Saline
6-OHDA DA-JC1
Week 4
Week 2
5-20rpm in 20 sec
Week 4

Fig. 4

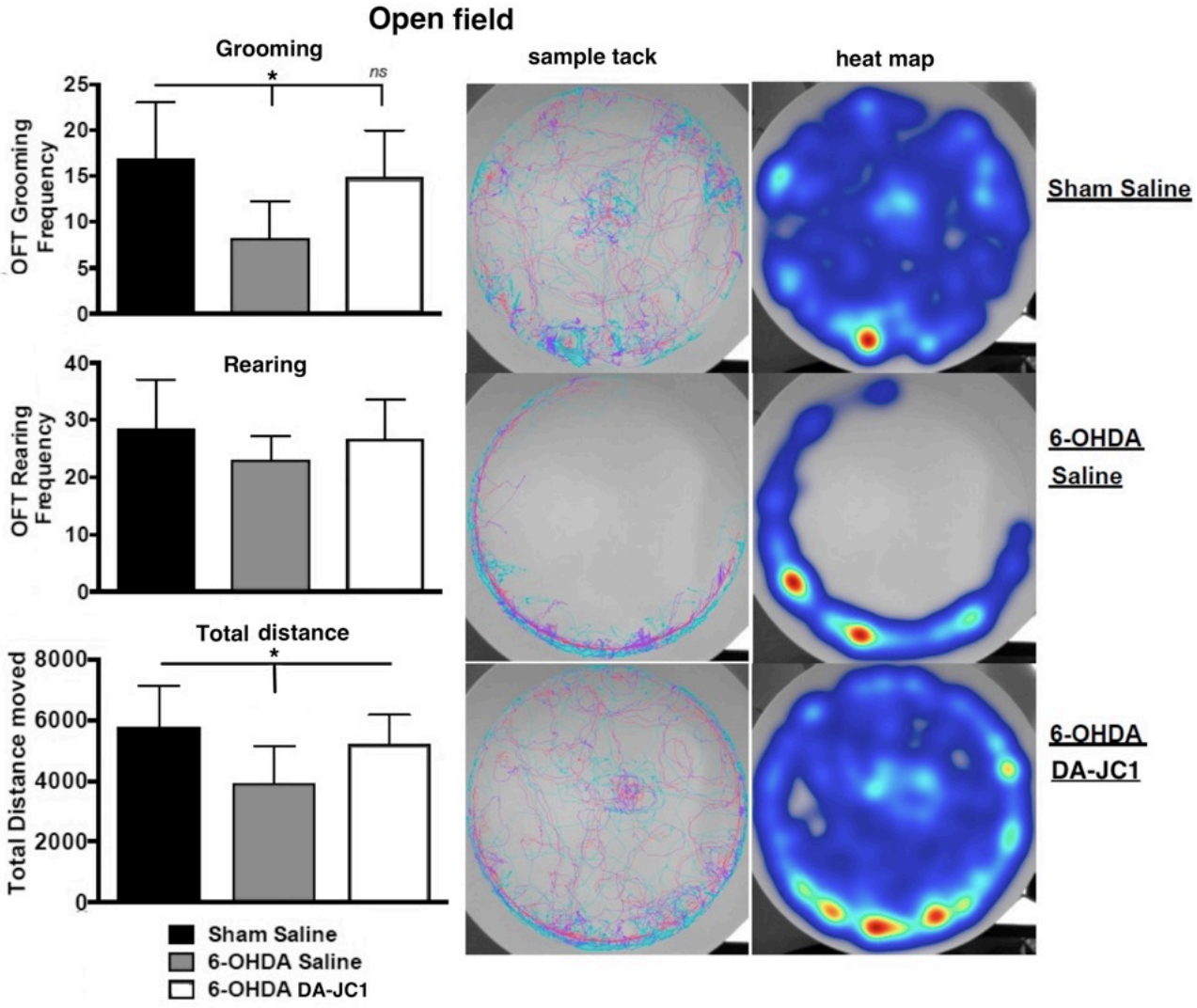
Open field
Grooming
*
ns
OFT Grooming Frequency
25
20
15
10
5
0
Rearing
OFT Rearing Frequency
40
30
20
10
0
Total distance
*
Total Distance moved
8000
6000
4000
2000
0
Sham Saline
6-OHDA Saline
6-OHDA DA-JC1
sample tack
heat map
Sham Saline
6-OHDA Saline
6-OHDA DA-JC1

Fig. 5

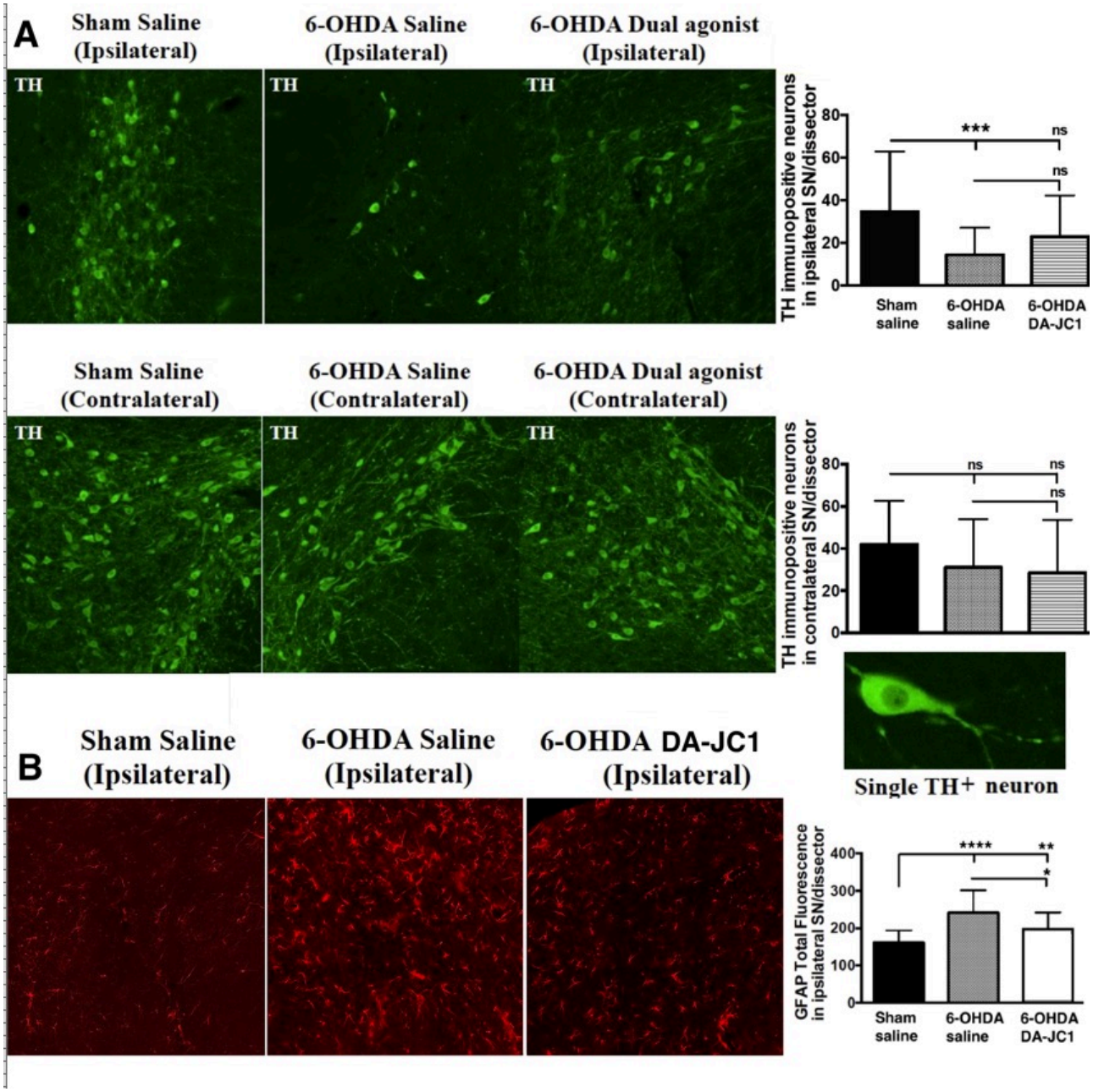
A
Sham Saline (Ipsilateral)
6-OHDA Saline (Ipsilateral)
6-OHDA Dual agonist (Ipsilateral)
TH
TH
TH
TH immunopositive neurons in ipsilateral SN/dissector
***
ns
ns
Sham saline
6-OHDA saline
6-OHDA DA-JC1
Sham Saline (Contralateral)
6-OHDA Saline (Contralateral)
6-OHDA Dual agonist (Contralateral)
TH
TH
TH
TH immunopositive neurons in contralateral SN/dissector
ns
ns
ns
Single TH+ neuron
B
Sham Saline (Ipsilateral)
6-OHDA Saline (Ipsilateral)
6-OHDA DA-JC1 (Ipsilateral)
GFAP Total Fluorescence in ipsilateral SN/dissector
****
**
*
Sham saline
6-OHDA saline
6-OHDA DA-JC1

Fig. 6

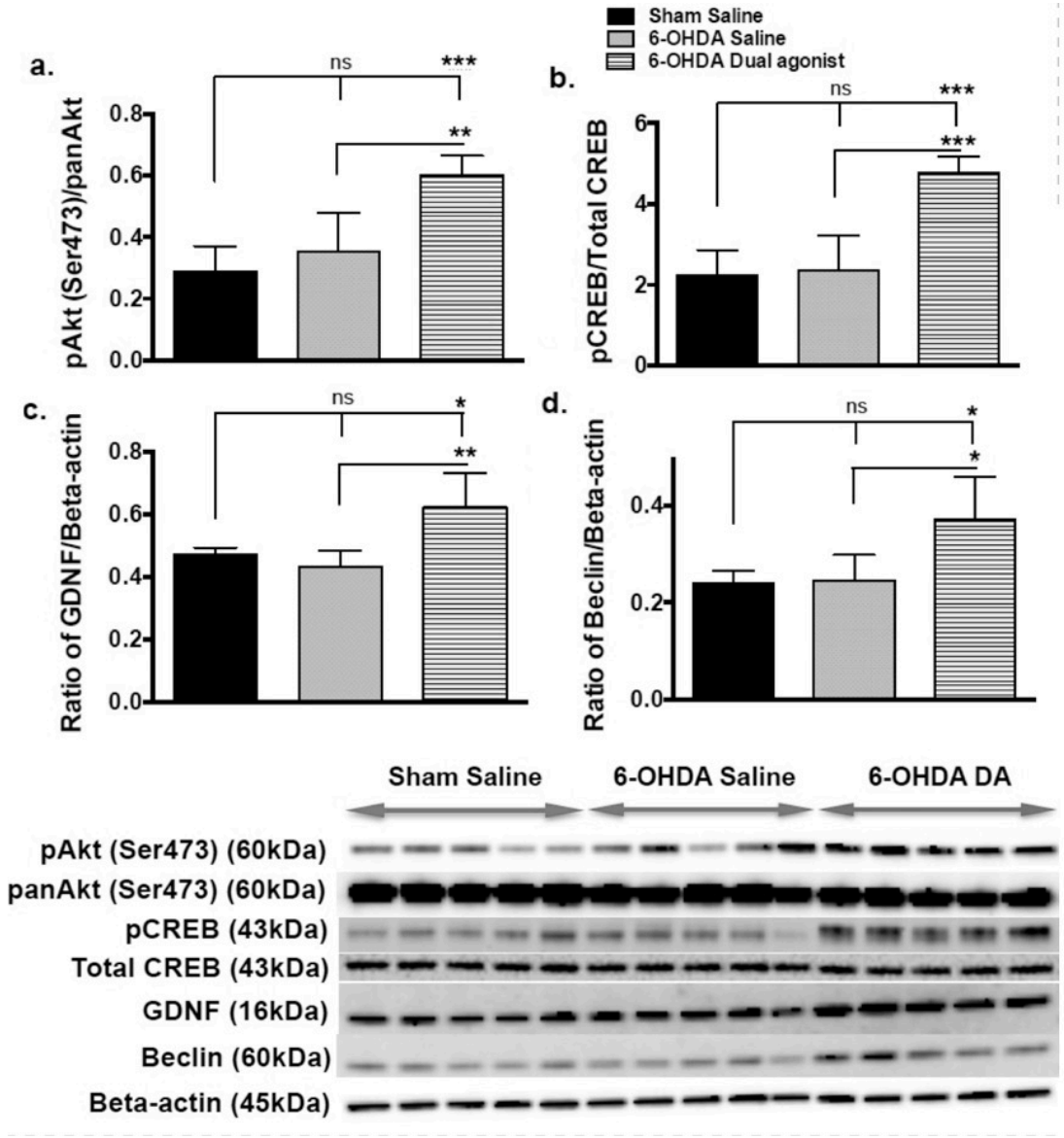
Sham Saline
6-OHDA Saline
6-OHDA Dual agonist
a.
pAkt (Ser473)/panAkt
ns
***
**
b.
pCREB/Total CREB
ns
***
***
c.
Ratio of GDNF/Beta-actin
ns
*
**
d.
Ratio of Beclin/Beta-actin
ns
*
*
Sham Saline
6-OHDA Saline
6-OHDA DA
pAkt (Ser473) (60kDa)
panAkt (Ser473) (60kDa)
pCREB (43kDa)
Total CREB (43kDa)
GDNF (16kDa)
Beclin (60kDa)
Beta-actin (45kDa)

Fig. 7

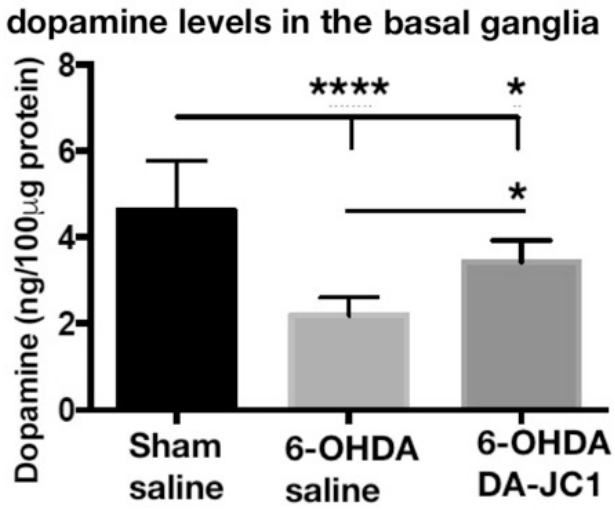
dopamine levels in the basal ganglia
Dopamine (ng/100μg protein)
8
6
4
2
0
****
*
*
Sham saline
6-OHDA saline
6-OHDA DA-JC1

fig. 8